CoS₂ Yolk-Shell Spheres Coated with Carbon Thin Layers as High Active and Stable Electrocatalysts for Hydrogen Evolution Reaction

Wang Anliang, *Tong Yexiang*, *Li Gaoren* *

MOE Laboratory of Bioinorganic and Synthetic Chemistry, The Key Lab of Low-Carbon Chemistry & Energy Conservation of Guangdong Province, School of Chemistry, Sun Yat-Sen University, Guangzhou 510275, P. R. China

Abstract: Though water electrolysis is effective in generating high-quality hydrogen gas, it requires effective electrocatalysts for hydrogen evolution reaction (HER). CoS_2 have been considered as a promising HER electrocatalyst because of its high ctalytic activity. However, the key limitation for CoS_2 nanomaterial as HER electrocatalyst is its poor stability, which may be due to the structural breakdown of CoS_2 nanostructure or the evolution of S during H_2 evolution in acid media. Coating porous carbon thin layer for protection from structural breakdown and evolution of S is a good way to improve catalytic stability. In addition, coating carbon layer can change electronic structure of CoS_2 for the moderated hydrogen adsorption energy, leading to enhanced catalytic activity. Here, CoS_2 yolk-shell spheres coated with carbon thin layers exhibit superior catalytic performance for HER with low overpotential, small Tafel slope, and excellent stability.

Key words: CoS_2@C; yolk-shell sphere; electrocatalyst; hydrogen evolution reaction (HER); high stability

CLC number: O646　　　**Document code:** A　　　**Article ID:** 1005-1120(2018)04-0619-11

0　Introduction

Hydrogen as a sustainable, secure, clean and alternative energy source can ease the energy crisis and environment pollution faced in the present world[1-2]. Electrochemical water splitting is considered as a highly effective method to produce hydrogen[3]. However, it needs electrocatalysts to reduce overpotential due to low kinetics of water splitting. Pt is at present the most active catalyst for the hydrogen evolution reaction (HER)[4-5]. However, its scarcity on the earth and high cost greatly restrict the industrial production of hydrogen. Therefore, it is necessary and urgent to find cost-effective and earth-abundant catalysts with high HER catalytic activity and excellent stability to facilitate translation of H_2O to hydrogen.

Transition metal dichalcogenides with gener- alized formula of MX_2 (M refers to transition metal; X represents a chalcogen such as S and Se) have received increasing interests due to their low cost and high abundance[6-10]. Among them, MoS_2 has been considered as a promising candidate because of its high activity and stability[11-14]. However, the experimental and computational studies have concluded that the catalytic activity mainly arises from the active sites located along the edges of 2-D MoS_2 layers which are under-co-ordinated and thermodynamically unfavorable, and the basal planes are catalytically inert[15-17]. Although various methods have been adapted to expose more edge sites or enhance the intrinsic activity of the edge sites, the enhancement of HER electrocatalytic performance of MoS_2 still faces enormous challenges[18-20]. Another transition metal dichalcogenides CoS_2, which was often utilized as electrode materials for supercapactiors,

Li-ion batteries or electrocatalysts for oxygen reduction reaction (ORR)[21-26], also has shown excellent HER electrocatalytic activity, even higher than MoS_2. In addition, CoS_2, which is an intriscally conductive metal in contrast to the other MX_2 such as FeS_2[27] and NiS_2[28], can improve the electron transportation from catalyst surface to the electrode, thus will reduce the overpotential needed to overcome the energy barriers and decrease the energy consumption. What's more, CoS_2 can exhibit high HER activity after conversion from thermodynamically favored semiconducting phase to a metastable metallic polymorph compared wih other transition metal dichalcogenideis, such as MoS_2 and WS_2[29-32]. However, the key limitation for CoS_2 as HER electrocatalyst is poor stability in acid media, which may be due to the structural breakdown of CoS_2 nanostructure or the evolution of S during H_2 evolution[24,33-37]. The poor stability of CoS_2 materials has seriously restricted their practical applications as high-performance HER electrocatalysts. Therefore, it is significant to develop CoS_2-based electrocatalysts with excellent stability as well as high catalytic activity.

To improve the electrocatalytic activity and stability of CoS_2 for HER, carbon thin layer coating will be a promising method because of following advantages: (1) the carbon thin layer can well prevent CoS_2 from structural breakdown and the evolution of S; (2) the electronic interaction between CoS_2 and thin carbon layer will change the electronic structure of CoS_2, which will be beneficial for the improvement of electrocatalytic activity; (3) The carbon layer will provide "superhighways" for electron transfer to promote HER

due to its high electrical conductivity. Based on the above considerations, we devote our attention to designing and synthesizing the novel CoS_2 yolk-shell (YS) spheres coated with carbon thin layers (CoS_2 YS@C spheres) as highly efficient HER electrocatalysts by a simple hydrothermal method. The CoS_2 YS@C spheres own hollow structure and high specific surface area, and they exhibit excellent catalytic activity with low onset potential of only about 20 mV, small Tafel slope of about 55 mV/dec, and small overpotential of about 90 mV at 10 mA/cm^2 in acidic solution. Especially, CoS_2 YS@C spheres also exhibit excellent stability at 10 mA/cm^2 for 10 h. This work provides a new revenue for the development of CoS_2-based electrocatalysts with high catalytic activity and excellent stability for HER.

1 Results and Discussion

Fig. 1 shows the schematic illustration of the fabrication of CoS_2 YS@C spheres. SEM images of CoS_2 YS spheres are shown in Figs. 2(a) and (b), which clearly shows that the diameters of CoS_2 YS spheres are about 2 μm and the surfaces of CoS_2 YS spheres are rough and made up of many small spheres. From the broken CoS_2 YS spheres, the YS structures are clearly seen as shown in Fig. 2(b), and the shell thickness is about 200 nm. This unique hollow and YS structures of CoS_2 will provide large surface areas, and they will be beneficial for the transportations of reactant and resultant and the enhancement of active sites. Then CoS_2 YS spheres coated with carbon thin layers (CoS_2 YS@C spheres) were achieved via hydrothermal treatment of CoS_2 YS spheres in glucose solution for 2 h. SEM image of
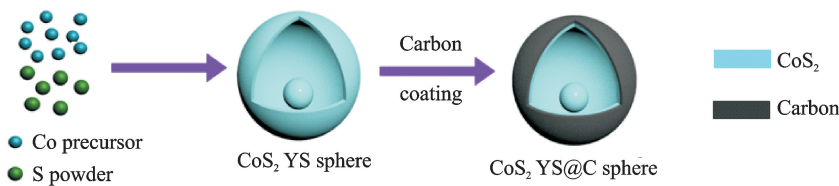

Fig. 1 Schematic of fabrication of CoS_2 YS@C spheres

(a) SEM image of CoS₂ YS spheres

(b) SEM image of broken CoS₂ YS spheres

(c) SEM image of CoS₂ YS@C spheres

(d) TEM image of CoS₂ YS@C spheres

(e) HRTEM image of Area ① in Fig.2(d) of CoS₂ YS@C sphere

(f) FFT pattern measured in Area ① in Fig.2(d)
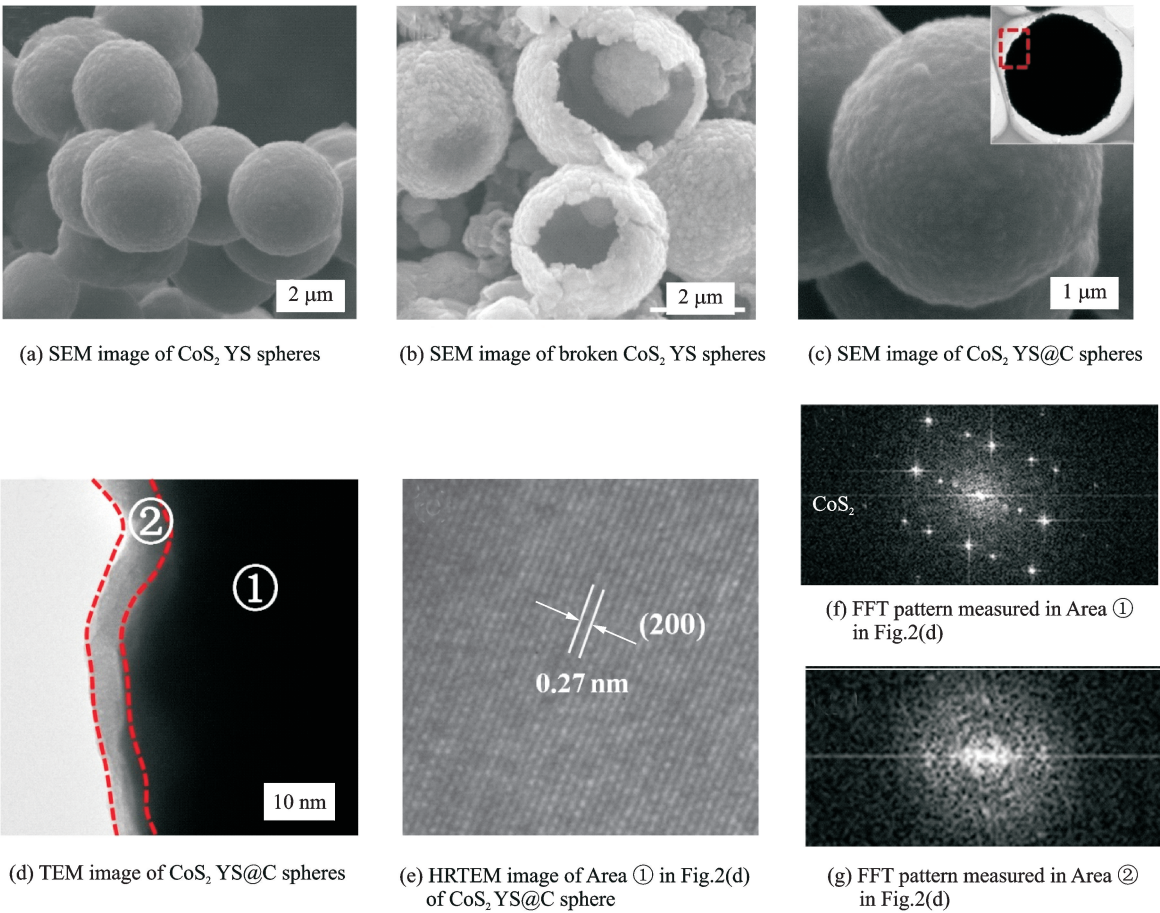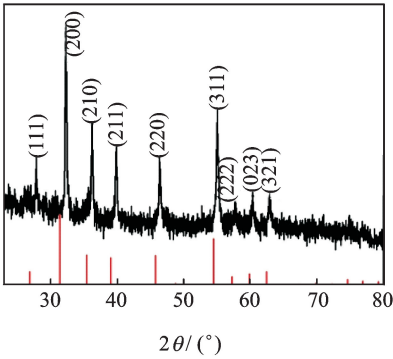

(g) FFT pattern measured in Area ② in Fig.2(d)

Fig. 2　SEM image of CoS₂ YS spheres，SEM image of broken CoS₂ YS spheres，SEM and TEM images of CoS₂ YS@C spheres，HRTEM image of Area① in Fig. 2(d) of CoS₂ YS@C sphere，FFT pattern measured in Area① in Fig. 2(d)，and FFT pattern measured in Area② in Fig. 2(d)

CoS₂ YS@C spheres in Fig. 2(c) shows carbon layers are unifromly coated on the surfaces of CoS₂ YS spheres. Compared with those of CoS₂ YS spheres, the surfaces of CoS₂ YS@C spheres become smoother because of the coating of carbon layer. To investigate the thickness of carbon layer, HRTEM image of the edge layer of CoS₂ YS @C is measured (Fig. 2(d)), which shows that the carbon layer is uniform with thickness of about 10 nm. Fig. 2(e) shows that the inner CoS₂ owns clear lattice fringes of about 0.226 nm, which corresponds to (200) plane of CoS₂, and fast Fourier transform (FFT) parttern in Fig. 2(f) indicates the single crystal structure of CoS₂. The carbon layer is amorphous structure without lattice fringe, and FFT parttern in Fig. 2(g) confirms the amorphous structure of carbon thin layer. XRD pattern of CoS₂ YS@C is shown in Fig. 3(a), which shows that all the diffraction
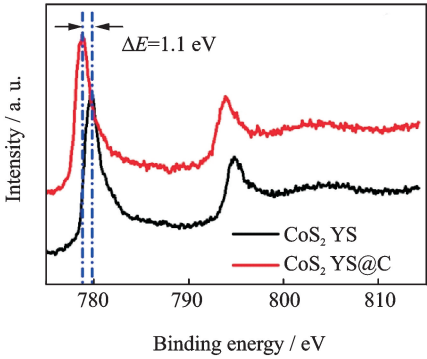
peaks are attributed to the standard cubic phase of CoS₂ (PDF 65-3322) and no diffraction peak of carbon is seen, furthermore confirming the crystalline structure of CoS₂ and amorphous structure of carbon layer. Here the thickness of carbon layer of CoS₂ YS @ C sphere can be well controlled. When the hydrothermal treatment time of CoS₂ YS spheres in glucose solution is 3 h, the surface of CoS₂ YS@C sphere is also uniform and the carbon layer is about 15 nm. When the hydrothermal treatment time of CoS₂ YS spheres in glucose solution is 1 h, the unifrom carbon layer is about 6 nm. In order to investigate the effect of carbon layer on the electronic structure of CoS₂, XPS measurements of CoS₂ YS spheres and CoS₂ YS@C spheres were performed. In Co 2p region (Fig. 3(b)), the peaks of Co 2p₁/₂ and 2p₃/₂ of CoS₂ YS@C spheres at 793.9 and 778.8 eV both shift to lower binding energy compared with those

of Co $2p_{1/2}$ and Co $2p_{3/2}$ of CoS_2 YS spheres at 795.0 and 779.9 eV, respectively, and the negetive shifts are about 1.1 eV. In S 2p region (Fig. 3 (c)), the peaks of S $2p_{1/2}$ and $2p_{3/2}$ of CoS_2 YS@C spheres at 163.14 and 164.24 eV both shift to higher binding energy compared with those of S $2p_{1/2}$ and S $2p_{3/2}$ of CoS_2 YS spheres at 162.70 and 163.80 eV, respectively, and the positive shifts are about 0.44 eV. The negative shifts of Co 2p peaks and positive shifts of S 2p peaks well confirm the change of electronic structure of CoS_2 because of the strong electronic interaction between CoS_2 and carbon layers. XPS spectrum of C 1s of carbon layers is shown in Fig. 3(d), and it can be deconvoluted into three peaks at 284.8, 285.9 and 288.9 eV, which correspond to the bonds of C—C, C—O—C and O—C=C, respectively. The existences of C—O and O—C=C bonds in carbon layers will make CoS_2 YS@C spheres more hydrophilic，which is beneficial for the absorption of H_2O for HER[38]. In addition，Raman measurements were used to investigate the effect of carbon layer on the electronic structure of CoS_2, and Raman spectra of CoS_2 and CoS_2 YS@
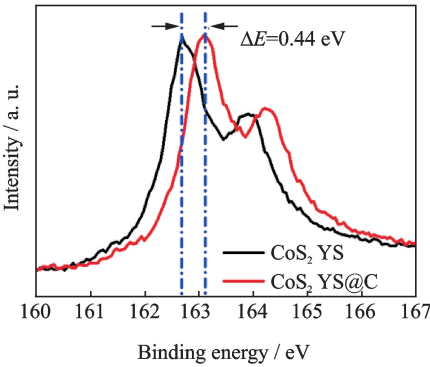
C spheres are shown in Fig. 3(c). The peaks at 293.5 and 398.6 cm^{-1} are observed for CoS_2, which correspond to the pure librational mode of dumb-bells (E_g) and in-phase stretching vibrations of S atom in the dumb-bells (A_g), respectively[39], and they are in agreement with the data of CoS_2 single crystal[21,40]. However，for CoS_2 YS@C，there are about 6 cm^{-1} negative shifts of E_g and A_g peaks (287.5 and 392.6 cm^{-1}) compared with those of CoS_2 YS spheres, as shown in Fig. 3(e)，further confirming the change of electronic structure of CoS_2 because of the strong electronic interaction between CoS_2 and carbon layers. To determine the content of C in CoS_2 YS@C sphere，TGA measurements of CoS_2 and CoS_2 YS@C spheres were studied in the air and the results are shown in Fig. 3(f). Compared with CoS_2, there is slow decrease among the temperature of 100—400 °C for CoS_2 YS@C，which corresponds to the lose of carbon in the sample. The compositions of C and CoS_2 in CoS_2 YS@C spheres are determined to be about 6% and 94% in weight，respectively.
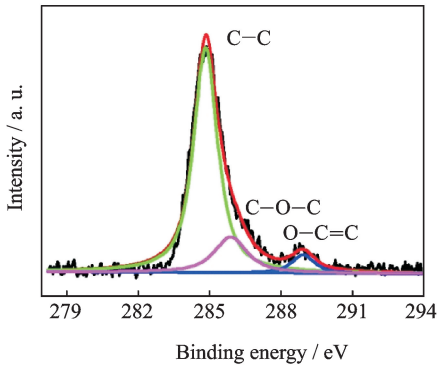

(a) XRD pattern of CoS_2 YS@C spheres

(b) XPS spectra of Co 2p region of CoS_2 YS and CoS_2 YS@C spheres

(c) XPS spectra of S 2p region of CoS_2 YS and CoS_2 YS@C spheres

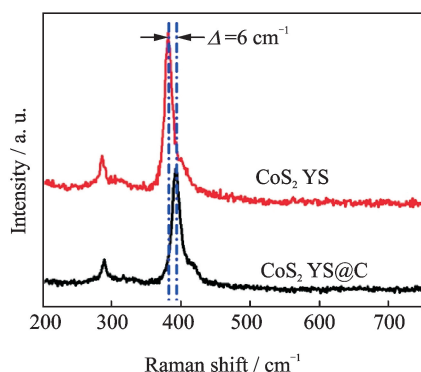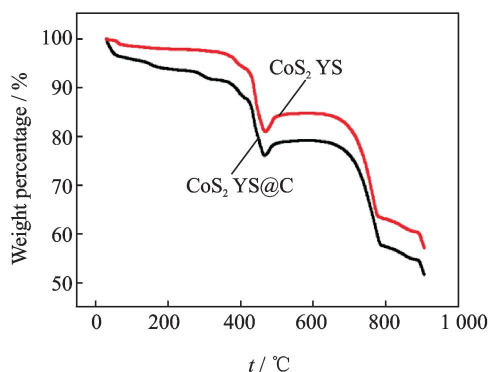(d) XPS spectra of C 1s region of CoS_2 YS@C spheres

(e) Raman spectra of CoS₂ YS and CoS₂ YS@C spheres   (f) TGA curves of CoS₂ YS and CoS₂ YS@C spheres

Fig. 3   XRD pattern of CoS₂ YS@C spheres，XPS spectra of Co 2p region of CoS₂ YS and CoS₂ YS@C spheres，XPS spectra of S 2p region of CoS₂ YS and CoS₂ YS@C spheres，XPS spectra of C 1s region of CoS₂ YS@C spheres，Raman spectra of CoS₂ YS and CoS₂ YS@C spheres，and TGA curves of CoS₂ YS and CoS₂ YS@C spheres

The electrocatalytic activities of CoS_2 YS@C spheres with different carbon layer thickness are studied by linear sweep voltammetry (LSV) in 0.5 M H_2SO_4 solution at 2 mV/s. When the carbon layer thickness is 10 nm, the electrocatalytic activity of CoS_2 YS@C spheres reaches the highest level (the carbon layer thickness of CoS_2 YS@C spheres was kept to be 10 nm in all the following experiments). The electrocatalytic activities of CoS_2 YS@C spheres，CoS_2 YS spheres and carbon with the same loadings (1.02 mg/cm²) were compared and their polarization curves are shown in Fig. 4(a). Obviously，the HER catalytic activity of CoS_2 YS@C is much better than that of CoS_2 YS spheres and the carbon almost has no catalytic activity. The onset potential of CoS_2 YS@C is about 20 mV，which is much lower than those of CoS_2 YS spheres (85 mV)，as shown in Fig. 4(b). The overpotential of CoS_2 YS@C at 10 mA/cm² is 89.3 mV，which is much smaller than 184.2 mV of CoS_2 YS spheres. In addition，the current density of CoS_2 YS@C at a given potential is much higher than that of CoS_2 YS spheres，as shown in Fig. 4(b). For instance，when the overpotential is 200 mV，the current density of CoS_2 YS@C spheres is about 81.23 mA/cm²，which is about 6.5 times higher than that of CoS_2 YS speheres，as shown in Fig. 4(c)，suggesting the important role of carbon thin layer for the enhancement of electrocatalytic
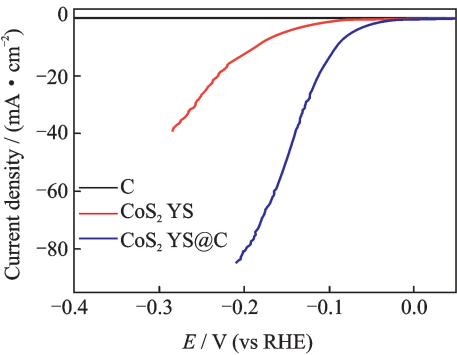
activity of CoS_2 YS@C speheres.

The linear portions of Tafel plots were fit to Tafel equation ($\eta = a + b\log j$，where j is current density，b is Tafel slope)，yielding Tafel slope of about 55 mV/dec for CoS_2 YS@C spheres (Fig. 4 (d))，which is much lower than that of CoS_2 (77 mV/dec). The Tafel slope of 55 mV/dec for CoS_2 YS@C indicates Volmer reaction has been taken place[41-42]，and the process to convert the protons into absorbed hydrogen atoms on CoS_2 YS @C surfaces becomes rate-determining step during HER. The exchange current density (j_0) of the catalyst can be calculated by extrapolating the Tafel plot. As expected，j_0 of CoS_2 YS@C spheres is 0.265 mA/cm² (Fig. 5(a))，which is much larger than that of CoS_2 (0.062 mA/cm²). Therefore，the CoS_2 YS@C spheres exhibit outstanding HER activity with low onset potential，high current density，low Tafel slope and high exchange current density，which are superior to most of the CoS_2-based electrocatalysts that have been ever reported in the acidic electrolyte.

In order to further provide the insight to CoS_2 YS@C sphere electrocatalysts，the electrochemical active surface area (ECSA) and electrochemical impedance spectroscopy (EIS) measurements were performed. Though it is difficult to obtain the accurate value of ECSA owing to the unclear capacitive behavior，it can be visualized by double layer capacitance (C_{dl})，which is pro-
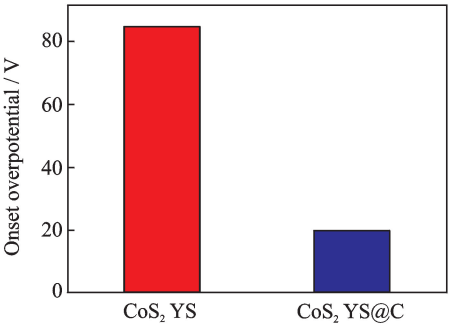
portional to the electrochemical surface area. The calculation of C_{dl} by cycle voltammograms (CVs) in 0. 5 M H_2SO_4 is used to make comparison of ECSA. The C_{dl} of CoS_2 YS@C spheres is caculated to be 13. 13 mF/cm^2 (Figs. 5(b) and (c)), which is much larger than that of CoS_2 YS spheres (6. 56 mF/cm^2), indicating that CoS_2 YS@C spheres own much larger ECSA than CoS_2 YS spheres. Nyquist plots of CoS_2 and CoS_2 YS@C spheres are shown in Fig. 5(d). The semicircle in the high frequency region is attributed to the charge transfer resistance (R_{ct}), which is related to the electrocatalytic kinetics, and a low value of semicircle is consistent with a fast reaction rate[43]. From Fig. 5(d), it is clearly seen that CoS_2 YS@C spheres have much lower R_{ct} than CoS_2 YS spheres, indicating much faster reaction rate for CoS_2 YS@C spheres.

HER electrocatalytic activity of CoS_2 YS@C spheres is significantly better than those of CoS_2
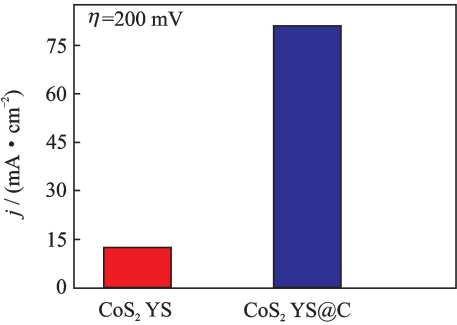
and other CoS_2-based electrocatalysts reported in the litertatures. The enhancement of the catalytic activity of CoS_2 YS@C spheres can be ascribed to the rapid charge transfer based on analyses of EIS results and the large ECSA with more exposed active sites. Actually the better catalytic activity of CoS_2 YS@C spheres as electrocatalysts for HER is also due to the natural properties of CoS_2 YS@ C spheres. As we all know, HER activity is strongly correlated with the chemisorption energy of atomic hydrogen to the electrocatalyst surface, and the hydrogen binding energy for an excellent HER electrocatalyst should be neither too high nor too low[44-45]. The positive hydrogen binding energy on CoS_2 indicates a weak adsorption of H on CoS_2 surface[45], which will be unfavourable to the reduction of H^+ (i. e., Volmer step). Thus, an optimization of the electronic features is desired. It is notable that the surrounding elements have an important effect on the electron density
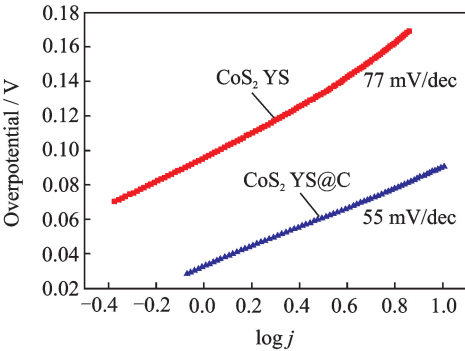

(a) IR-corrected polarization curves of CoS_2 YS spheres, CoS_2 YS@C spheres, and C in 0.5 M H_2SO_4 at 2 mV/s

(b) Comparisons of the onset overpotentials of CoS_2 YS and CoS_2 YS@C spheres

(c) Comparisons of HER current densities of CoS_2 YS and CoS_2 YS@C spheres at the overpotential of 200 mV

(d) Tafel plots of CoS_2 YS and CoS_2 YS@C spheres

Fig. 4   IR-corrected polarization curves of CoS_2 YS spheres, CoS_2 YS@C spheres, and C in 0. 5 M H_2SO_4 at 2 mV/s; comparisons of the onset overpotentials of CoS_2 YS and CoS_2 YS@C spheres; comparisons of HER current densities of CoS_2 YS and CoS_2 YS@C spheres at the overpotential of 200 mV; and Tafel plots of CoS_2 YS and CoS_2 YS@C spheres
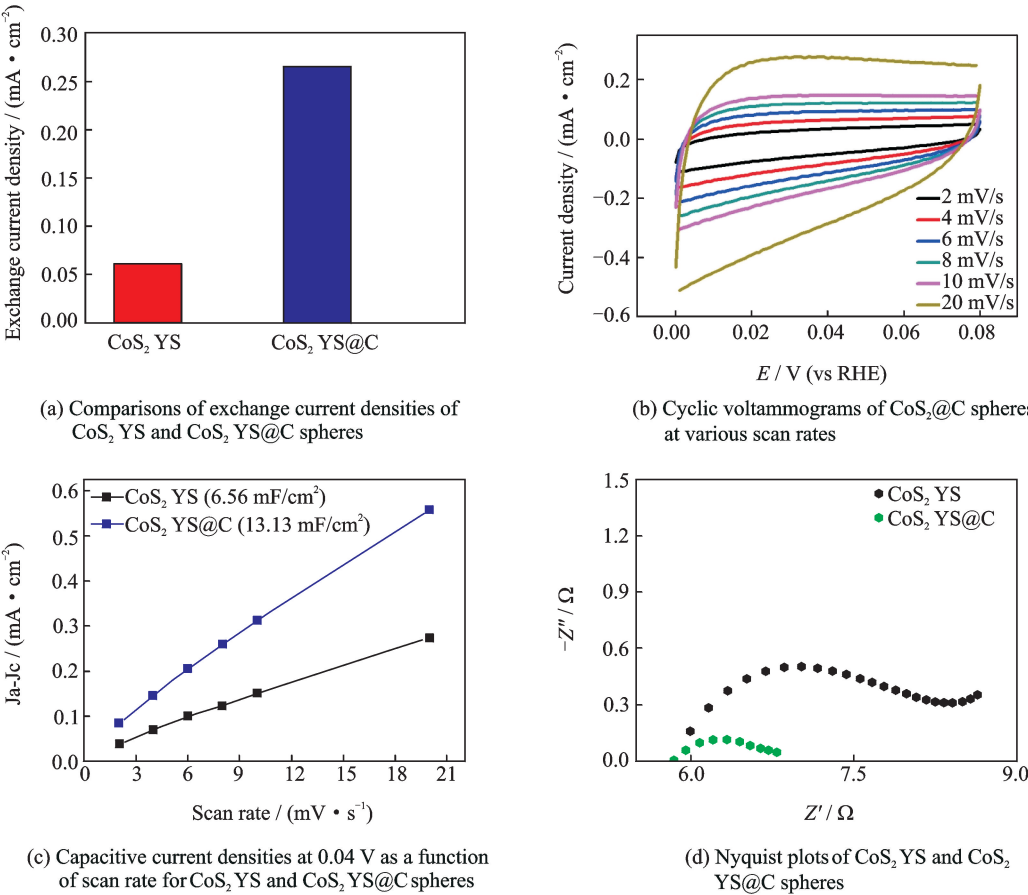
(a) Comparisons of exchange current densities of CoS₂ YS and CoS₂ YS@C spheres

(b) Cyclic voltammograms of CoS₂@C spheres at various scan rates

(c) Capacitive current densities at 0.04 V as a function of scan rate for CoS₂ YS and CoS₂ YS@C spheres

(d) Nyquist plots of CoS₂ YS and CoS₂ YS@C spheres

Fig. 5 Comparisons of exchange current densities of CoS₂ YS and CoS₂ YS@C spheres, cyclic voltammograms of CoS₂ @C spheres at various scan rates, capacitive current densities at 0.04 V as a function of scan rate for CoS₂ YS and CoS₂ YS@C spheres, and nyquist plots of CoS₂ YS and CoS₂ YS@C spheres
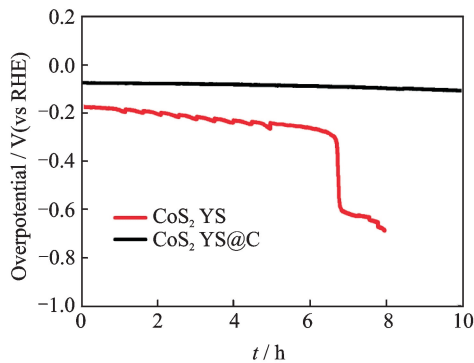
around Co active sites. As we all know, carbon has a lower electronegativity compared with S, so the electron density around Co will increase by embedding carbon onto the surface of CoS₂. This phenomenon has been well demonstrated by XPS and Raman results. XPS binding energy of Co 2p of CoS₂ YS@C spheres obviously decreases compared with that of CoS₂, as shown in Fig. 3(b), indicating that the valence of Co in CoS₂ YS@C shperes is below +2 and the electronic density of Co will increase. In addition, E_g and A_g peaks of CoS₂ YS@C spheres shifting to low Raman shift compared with that of CoS₂ YS spheres also confirms the strong electronic interactions between CoS₂ and carbon thin layer, as shown in Fig. 3(e). Therefore, the increase of electronic density of Co will consequently enhance the strength of hydrogen binding energy to promote H_{ads} adsorption and thus will improve HER cata-

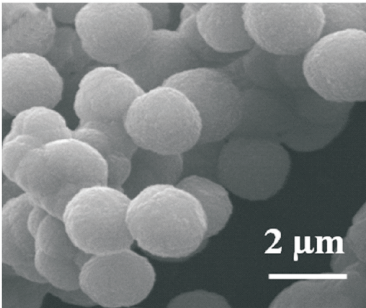lytic activity of CoS₂ YS@C spheres.

Besides the HER electrocatalytic activity, the stability is also one important criterion in evaluating the performance of electrocatalyst. The long-term HER electrocatalytic stabilities of CoS₂ YS spheres and CoS₂ YS@C spheres were tested through continuous electrolysis at 10 mA/cm² in 0.5 M H₂SO₄ for 10 h. As shown in Fig. 6(a), it is clearly seen that the CoS₂ YS@C spheres exhibit high durability with slight overpotential increase of about 32 mV at 10 mA/cm² after 10 h, whereas CoS₂ YS spheres exhibit very poor durability with obvious overpotential increase of about 517 mV after 8 h. To further gain insight into the stability of electrocatalysts, CoS₂ YS spheres and CoS₂ YS@C spheres after stability tests were further studied by SEM and XPS. It is observed that the surface morphology of CoS₂ YS@C still remains very well after stability tests, as shown in

Fig. 6(b). However, for CoS$_2$ YS spheres, their surface morphology is seriously damaged after stability tests. So here the carbon thin layer plays a very important role for the protection from structural breakdown of CoS$_2$ YS@C spheres, as illustrated in Fig. 6(e). XPS characterization was also performed on CoS$_2$ and CoS$_2$ YS@C spheres after stability tests. It is clearly seen that the XPS peaks of 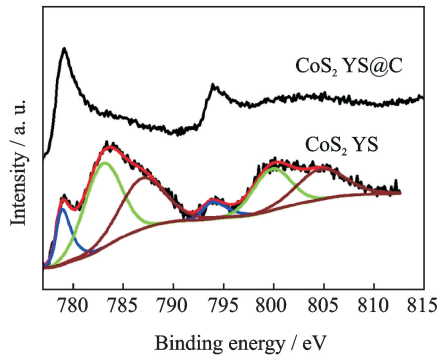Co 2p of CoS$_2$ YS@C spheres al-most remain unchangeable compared with those of CoS$_2$ YS@C spheres before stablity tests, suggesting high chemical stability of CoS$_2$ YS@C spheres. However, for CoS$_2$ YS spheres, besides the peaks at 778.8 and 794.0 eV of Co 2p, two large new peaks appear at 783.1 and 799.9 eV, as shown in Fig. 6(c), which can be attributed to other forms of Co because of the oxidation of CoS$_2$. In addition, for CoS$_2$ YS spheres, a large
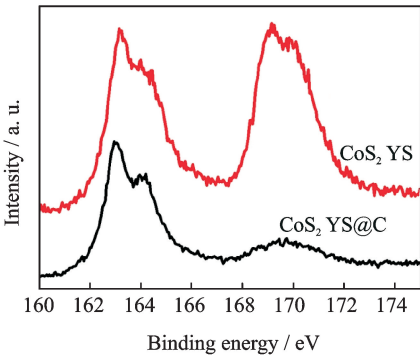

(a) Stability tests of CoS$_2$ YS and CoS$_2$ YS@C spheres at 10 mA/cm^2
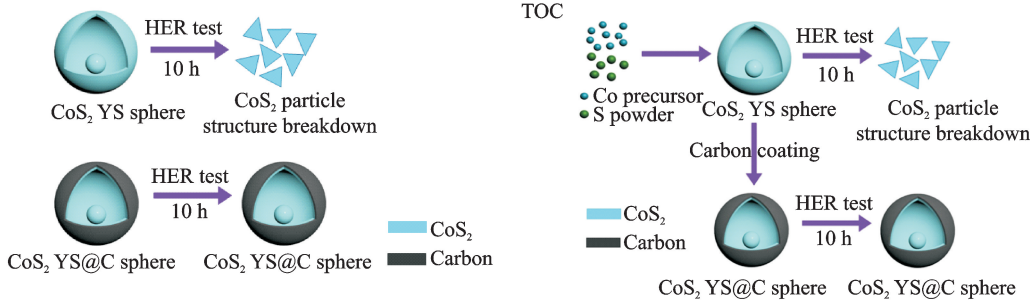

(b) SEM image of CoS$_2$ YS@C spheres after stability tests for 10 h

(c) XPS spectra of CoS$_2$ YS and CoS$_2$ YS@C spheres in Co 2p region after stability tests for 10 h

(d) XPS spectra of CoS$_2$ YS and CoS$_2$ YS@C spheres in S 2p region after HER tests for 10 h

(e) Schematic of the advantage of CoS$_2$ YS@C spheres for long-term HER

Fig. 6   Stability tests of CoS$_2$ YS and CoS$_2$ YS@C spheres at 10 mA/cm^2, SEM image of CoS$_2$ YS@C spheres after HER test for 10 h, XPS spectra of CoS$_2$ YS and CoS$_2$ YS@C spheres in Co 2p region after HER tests for 10 h, XPS spectra of CoS$_2$ YS and CoS$_2$ YS@C spheres in S 2p region after HER test for 10 h, and schematic of the advantage of CoS$_2$ YS@C spheres for long-term HER

peak appears at 169. 2 eV in S 2p region, as shown in Fig. 6(d), indicating the evolution of S from CoS_2. However, for CoS_2 YS@C spheres, the oxidation of CoS_2 or the evolution of S are not observed as shown in Figs. 6(c) and (d). There fore, after coating carbon thin layers, CoS_2 YS@ C spheres can efficiently prevent from the structural breakdown, CoS_2 oxidation or S evolution, which all are beneficial for the improvements of catalytic activity and stability.

2　Conclusions

CoS_2 YS spheres coated with carbon thin layers (CoS_2 YS@C spheres) were designed and fabricated as high-performance electrocatalysts for HER in acid media. The unique YS structure provides large space for the reactant and resultant, which is beneficial for the improvement of utilization of active sites. The carbon thin layer coating can efficently change the electronic structure of CoS_2 for the appropriate hydrogen adsorption energy to promote the Volmer step of HER, and it also can protect CoS_2 from the structural breakdown and can prevent the evolution of S from CoS_2 for the improvement of elelctrocatalytic activity and stability. Because of the above advantages, CoS_2 YS@C spheres exhibit superior catalytic activity with low onset potential of about 20 mV, small Tafel slope of about 55 mV/dec, and small overpotential of about 90 mV at 10 mA/cm². Especially, CoS_2 YS@C spheres also exhibit high durability with overpotential increase of only about 8% at 10 mA/cm² for 10 h. This work provides a new avenue for the design of high-performance electrocatalysts that are unstable during the catalysis process.

References:

[1] KUANG Y, FENG G, LI P, et al. Single-crystalline ultrathin nickel nanosheets array from in situ topotactic reduction for active and stable electrocatalysis [J]. Angewandte Chemie International Edition, 2016, 55(2):693-697.

[2] DENG J, REN P, DENG D, et al. Highly active and durable non-precious-metal catalysts encapsulated in carbon nanotubes for hydrogen evolution reaction [J]. Energy Environment Science, 2014, 7 (6): 1919-1923.

[3] ZHANG Y, OUYANG B, XU J, et al. Rapid synthesis of cobalt nitride nanowires: Highly efficient and low-cost catalysts for oxygen evolution[J]. Angew Chem Int Ed Engl, 2016,55(30):8670-8674.

[4] WALTER M G, WARREN E L, MCKONE J R, et al. Solar water splitting cells[J]. Chemical Review, 2010, 110(11):6446-6473.

[5] BU L, GUO S, ZHANG X, et al. Surface engineering of hierarchical platinum-cobalt nanowires for efficient electrocatalysis [J]. Nature Communcations, 2016,7:11850.

[6] CHANG K, HAI X, PANG H, et al. Targeted synthesis of 2H- and 1T-phase MoS₂ monolayers for catalytic hydrogen evolution[J]. Advanced Materials, 2016, 28(45):10033.

[7] WANG D Y, GONG M, CHOU H L, et al. Highly active and stable hybrid catalyst of cobalt-doped FeS₂ nanosheets-carbon nanotubes for hydrogen evolution reaction[J]. Journal of the American Chemical Society, 2015, 137(4):1587-1592.

[8] KONG D S, WANG H T, LU Z Y, et al. CoSe₂ nanoparticles grown on carbon fiber paper: An efficient and stable electrocatalyst for hydrogen evolution reaction[J]. Journal of the American Chemical Society, 2014,136(13):4897-4900.

[9] ZHOU H, WANG Y, HE R, et al. One-step synthesis of self-supported porous NiSe₂/Ni hybrid foam: An efficient 3D electrode for hydrogen evolution reaction [J]. Nano Energy, 2016,20:29-36.

[10] LONG X, LI G, WANG Z, et al. Metallic iron-nickel sulfide ultrathin nanosheets as a highly active electrocatalyst for hydrogen evolution reaction in acidic media[J]. Journal of the American Chemical Society, 2015, 137(37):11900-11903.

[11] VOIRY D, SALEHI M, SILVA R, et al. Conducting MoS₂ nanosheets as catalysts for hydrogen evolution reaction[J]. Nano Letters, 2013, 13 (12): 6222-6227.

[12] WANG H, LU Z, KONG D, et al. Electrochemical

tuning of MoS_2 nanoparticles on three-dimensional substrate for efficient hydrogen evolution[J]. ACS Nano, 2014,8(5):4940-4947.

[13] LIAO L, ZHU J, BIAN X J, et al. MoS_2 formed on mesoporous graphene as a highly active catalyst for hydrogen evolution[J]. Advanced Functional Materials, 2013, 23(42):5326-5333.

[14] LI Y, WANG H, XIE L, et al. MoS_2 nanoparticles grown on graphene: An advanced catalyst for the hydrogen evolution reaction[J]. Journal of the American Chemical Society, 2011,133(19):7296.

[15] HINNEMANN B, MOSES P G, BONDE J, et al. Biomimetic hydrogen evolution: MoS_2 nanoparticles as catalyst for hydrogen evolution[J]. Journal of the American Chemical Society, 2005, 127 (15): 5308-5309.

[16] JARAMILLO T F, JØRGENSEN K P, BONDE J, et al. Identification of active edge sites for electrochemical H_2 evolution from MoS_2 nanocatalysts[J]. Science, 2007,317(5834):100-102.

[17] TSAI C, ABILD-PEDERSEN F, NØRSKOV J K. Tuning the MoS_2 edge-site activity for hydrogen evolution via support interactions [J]. Nano Letters, 2014, 14(3):1381-1387.

[18] XIE J, ZHANG H, LI S, et al. Defect-rich MoS_2 ultrathin nanosheets with additional active edge sites for enhanced electrocatalytic hydrogen evolution[J]. Advanced Materials, 2013,25(40):5807-5813.

[19] XIE J, ZHANG J, LI S, et al. Controllable disorder engineering in oxygen-incorporated MoS_2 ultrathin nanosheets for efficient hydrogen evolution[J]. Journal of the American Chemical Society, 2013,136(4):17881-17888.

[20] YANG Y, FEI H, RUAN G, et al. Edge-oriented MoS_2 nanoporous films as flexible electrodes for hydrogen evolution reactions and supercapacitor devices [J]. Advanced Materials, 2014, 26(48):8163-8168.

[21] ZHU L, SUSAC D, TEO M, et al. Investigation of CoS_2-based thin films as model catalysts for the oxygen reduction reaction[J]. Journal of Catalysis, 2008,258(1):235-242.

[22] WANG Q, JIAO L, HAN Y, et al. CoS_2 hollow spheres: Fabrication and their application in lithium-ion batteries[J]. Journal of Physical Chemistry C, 2011,115(16):8300-8304.

[23] JIRKOVSKÝ J S, BJÖRLING A, AHLBERG E. Reduction of oxygen on dispersed nanocrystalline CoS_2 [J]. Journal of Physical Chemistry C, 2012, 116 (46):24436-24444.

[24] FABER M S, DZIEDZIC R, LUKOWSKI M A, et al. High-performance electrocatalysis using metallic cobalt pyrite (CoS_2) micro- and nano-structures[J]. Journal of the American Chemical Society, 2014,136 (28):10053-10061.

[25] ZHANG H, LI Y, ZHANG G, et al. A metallic CoS_2 nanopyramid array grown on 3D carbon fiber paper as an excellent electrocatalyst for hydrogen evolution[J]. Journal of Materials Chemistry A, 2015 (3):6306-6310.

[26] XIE J, LIU S, CAO G, et al. Self-assembly of CoS_2/graphene nanoarchitecture by a facile one-pot route and its improved electrochemical Li-storage properties[J]. Nano Energy, 2013,2(1):49-56.

[27] CABÁN-ACEVEDO M, FABER M S, TAN Y, et al. Synthesis and properties of semiconducting iron pyrite (FeS_2) nanowires[J]. Nano Letters, 2012,12 (4):1977-1982.

[28] THIO T, BENNETT J. Hall effect and conductivity in pyrite NiS_2 [J]. Physical Review B, 1994, 50 (50):10574-10577.

[29] LUKOWSKI M A, DANIEL A S, MENG F, et al. Enhanced hydrogen evolution catalysis from chemically exfoliated metallic MoS_2 nanosheets[J]. Journal of the American Chemical Society, 2013,135(28):10274-10277.

[30] WANG H, LU Z, XU S, et al. Electrochemical tuning of vertically aligned MoS_2 nanofilms and its application in improving hydrogen evolution reaction[J]. Proceedings of the National Academy of Sciences, 2013,110(49):19701-19706.

[31] VOIRY D, YAMAGUCHI H, LI J, et al. Enhanced catalytic activity in strained chemically exfoliated WS_2 nanosheets for hydrogen evolution [J]. Nature Materials, 2013, 12:850-885.

[32] LUKOWSKI M A, DANIEL A S, ENGLISH C R, et al. Highly active hydrogen evolution catalysis from metallic WS_2 nanosheets[J]. Energy & Environmental Science, 2014,7(8):2608-2613.

[33] STASZAK-JIRKOVSKY J, MALLIAKAS C D, LOPES P P, et al. Design of active and stable Co-Mo-S_x chalcogels as pH-universal catalysts for the hydrogen evolution reaction[J]. Nature Materials, 2015,15(2):197-203.

[34] LUO W, XIE Y, WU C, et al. Spherical CoS_2 @ carbon core-shell nanoparticles: One-pot synthesis and Li storage property[J]. Nanotechnology, 2008, 19(7):075602.

[35] LIU H, LI W, SHEN D, et al. Graphitic carbon conformal coating of mesoporous TiO_2 hollow spheres for high-performance lithium ion battery an-

odes[J]. Journal of the American Chemical Society, 2015,137(40):13161-13166.

[36] LU X, LIU T, ZHAI T, et al. Improving the cycling stability of metal-nitride supercapacitor electrodes with a thin carbon shell[J]. Advanced Energy Materials, 2014,4(4):1300994.

[37] LIU T, FINN L, YU M, et al. Polyaniline and polypyrrole pseudocapacitor electrodes with excellent cycling stability[J]. Nano Letters, 2014,14(5):2522-2527.

[38] PENG S, LI L, MHAISALKAR S G, et al. Hollow nanospheres constructed by CoS$_2$ nanosheets with a nitrogen-doped-carbon coating for energy-storage and photocatalysis[J]. ChemSusChem, 2014,7(8):2212-2220.

[39] LYAPIN S G, UTYUZH A N, PETROVA A E, et al. Raman studies of nearly half-metallic ferromagnetic CoS$_2$[J]. Journal of Physics Condensed Matter An Institute of Physics Journal, 2014,26(39):396001.

[40] ANASTASSAKIS E, PERRY C. Light scattering and IR measurements in XS$_2$ pryite-type compounds [J]. Journal of Chemical Physics, 1976,64(9):3604-3609.

[41] MORALES-GUIO C G, STERN L A, HU X. Nanostructured hydrotreating catalysts for electrochemical hydrogen evolution[J]. Chemical Society Reviews, 2014,43(18):6555-6569.

[42] VILEKAR S A, FISHTIK I, DATTA R. Kinetics of the hydrogen electrode reaction[J]. Chemical Engineering Faculty Publications, 2010,157(7):B1040-B1050.

[43] MERKI D, VRUBEL H, ROVELLI L, et al. Fe, Co, and Ni ions promote the catalytic activity of amorphous molybdenum sulfide films for hydrogen evolution [J]. Chemical Science, 2012,3(8):2515-

2525.

[44] NØRSKOV J K, BLIGAARD T, LOGADOTTIR A, et al. Trends in the exchange current for hydrogen evolution[J]. Cheminform, 2005,36(8):e12154.

[45] CABÁN-ACEVEDO M, STONE M L, SCHMIDT J, et al. Efficient hydrogen evolution catalysis using ternary pyrite-type cobalt phosphosulphide[J]. Nature Materials, 2015,14(12):1245-1251.

Dr. **Wang Anliang** received the B. S. degree in Chemistry from Shandong Agricultural University in 2011 and the Ph. D. degree in Chemistry from Sun Yat－Sen in 2016, respectively. From 2016 to present, he has been a postdoctoral research fellow in Nanyang Technological University, Singapore. His research is focused on the design and synthesis of novel nanomaterials for electrocatalysis.

Prof. **Tong Yexiang** received his B. S. degree in General Chemistry in 1985, M. S. degree in Physical Chemistry in 1988, and Ph. D. degree in Organic Chemistry in 1999 from Sun Yat-Sen University. He joined Sun Yat-Sen University as assistant professor of Chemistry in 1988. He was granted the Talents Cultivated by "Thousand-Hundred-Ten" Program of Guangdong Province in 1996, the Secretary-General of Guangdong Chemical Society in 2009, and the councilman Chinese Chemical Society in 2010. His current research focuses on the electrochemical synthesis of alloys, intermetallic compounds and metal oxides nanomaterials and investigation of their applications for energy conversion and storage.

Prof. **Li Gaoren** received his B. S. degree in Applied Chemistry in 2000 from East China Institute of Technology and Ph. D. degree in Physical Chemistry in 2005 from Sun Yat-Sen University. He joined Sun Yat-Sen University as assistant professor of Chemistry in 2005. His current research focuses on the design and synthesis of novel electrocatalysts for water splitting and fuel cells.

(Production Editor：Xu Chengting)

Supporting Information
CoS₂ Yolk-Shell Spheres Coated with Carbon Thin Layers as High Active and Stable Electrocatalysts for Hydrogen Evolution Reaction

Wang Anliang，*Tong Yexiang*，*Li Gaoren*

MOE Laboratory of Bioinorganic and Synthetic Chemistry，KLGHEI of Environment and Energy Chemistry，School of Chemistry and Chemical Engineering，Sun Yat-sen University，Guangzhou 510275，P. R. China

Experimental Sections

The synthesis of CoS₂ spheres

CoS_2 spheres were synthesized according to the previous study reported by Lifang Jiao and her collabora-tors.[1] The details are listed as following: 1. 65 mmol of $CoCl_2$ $6H_2O$ was dissolved in absolute ethanol and then was transferred into a 40 mL Teflon-lined stainless steel autoclave，then 4. 1 mmol of sulfur powder was added into above solution. The Teflon-lined stainless steel auto-clave was subsequently stirred for 30 min. The sealed tank was maintained at 240 oC for 24 h. After reaction was over，the autoclave cooled to the room temperature naturally. The precipitati-ons were washed by ethanol three times and by distilled water one time and were collected by centrifugation. Finally，CoS_2 yolk-shell（YS） spheres were obtained after drying at 45 oC for 12 h.

The synthesis of CoS₂＠C spheres

The synthesized CoS_2 YS spheres（60 mg） were added into 30 ml 0. 05 M glucose solution and then were transferred into a 40 mL Teflon-lined stainless steel autoclave and the sealed tank was maintained at 180 ℃ for 2 h. After reaction，the autoclave cooled to the room temperature nat-urally. The precipitations were collected by cen-trifugation and washed by ethanol and distilled water，respectively. Finally，CoS_2 YS ＠ C spheres were obtained after drying at 45℃ for 12 h. For comparisons，the different hydrothermal time，such as 1 h and 3 h，was also used for the fabrication of CoS_2＠C with different thickness of carbon layer.

Material characterizations

The scanning electron microscope（SEM） and transition electron microscope（TEM） were undertaken on FEI Quanta 400 and FEI Tecnai G2 F30. Energy dispersive spectrum（EDS） map-ping was investigated by INCA 300. X-ray pow-der diffraction（XRD） analysis was performed on Bruker D8 diffractometer using Cu_α^K radiation. X-ray photoelectron spectroscopy（XPS） was pro-cessed using an ESCALAB X-ray photo-electron spectrometer. All XPS spectra were corrected u-sing the C 1s line at 284. 6 eV，and curve fitting and background subtraction were accomplished. The Fourier transform Raman（FT-Raman） spec-trum was achieved on the Nicolet NXR 9650.

Electrochemical tests

CoS_2＠C electrocatalysts were loaded on the glassy carbon electrode（GCE，diameter: 5mm） for testing in 0. 5 M H_2SO_4 using three-electrode system. Saturated calomel electrode（SCE） and graphite rod were used as reference and counter e-lectrodes，respectively. Typically，10 mg cata-lysts and 20 μl 5％ Nafion solution were dispersed in 0. 48 ml ethanol through 30 min ultrasound to form homogeneous ink. For the tests，10 μl cata-lyst ink was loaded onto the surface of GCE （loading 1. 02 mg • cm^{-2}）. All the potentials in this paper were referenced to a reversible hydro-gen electrode（RHE） by following equation:

$$E(RHE)＝E(SCE)＋0. 241＋0. 059 \text{ pH} \quad (1)$$

Before measurements，the solution was purged with N_2 for 10 min to pip out O_2 dissolved in the solution. HER electrocatalytic activity of CoS_2 YS＠C spheres was studied by linear sweep

voltammetry（LSV）at the scan rate of 2 mV • s^{-1}. Double layer capacitance（C_{dl}）was measured by CVs using the same working electrode at the potential window of 0. 19—0. 27 V vs SCE. CVs were obtained at different scan rates of 2，4，6，8，10，20 mV • s^{-1}. After plotting charging current density difference（$\Delta j = j_a - j_c$ at the current density of 0. 23 V）vs the scan rates，the slope，which is twice of C_{dl}，is used to represent ESCA. The chronopotentio-metry at 10 mA • cm^{-2} was mesured to test the stability of CoS_2 YS@C spheres. The EIS measurements were conducted at overpotential of 0. 24 V with the frequency ranging from 100 kHz to 0. 1 Hz. For comparisons，bare C，CoS_2 and the physical mixture of $CoS_2 +$ C（with the same ratio of CoS_2 and C as that of CoS_2 YS@C spheres）were also mixed with Nafion solution and ethanol to form homogenous ink，respectively，and they were loaded onto the surface of GCE with the same loadings of 1. 02 mg • cm^{-2}. The same tests of C，CoS_2 and CoS_2 +C as those of CoS_2@C spheres were also measured.
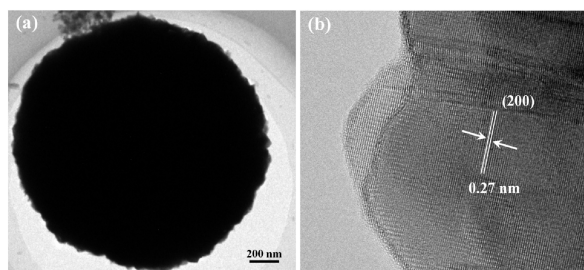

Fig. S1 （a）TEM image of CoS_2 YS sphere；（d）HRTEM image of CoS_2 sphere
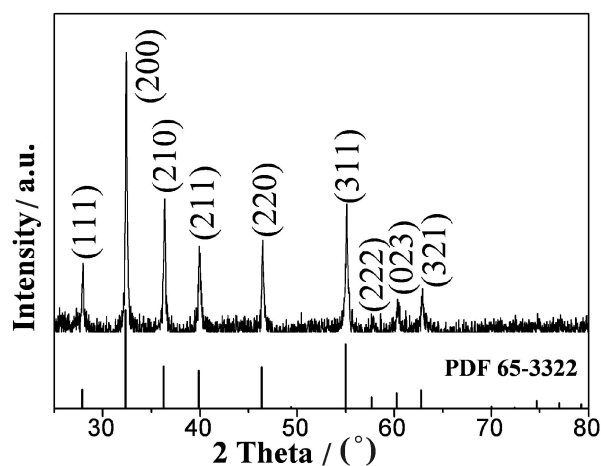

Fig. S2 XRD pattern of CoS_2 spheres

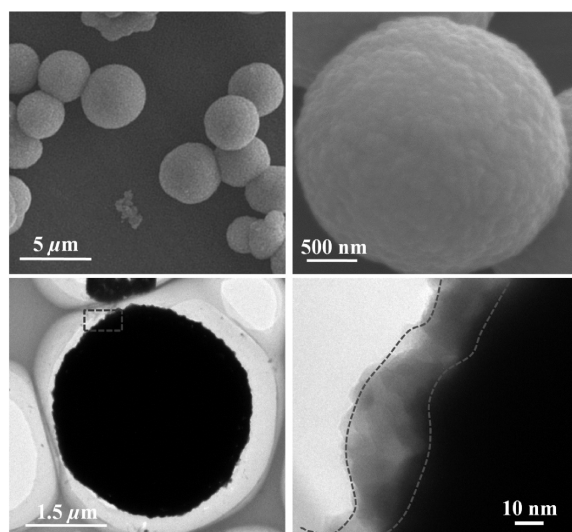Fig. S3 （a）SEM images of CoS_2 YS@C spheres with different magnifications；（c）TEM image of CoS_2 YS@C spheres and （d）HRTEM image of the wall of CoS_2@C sphere
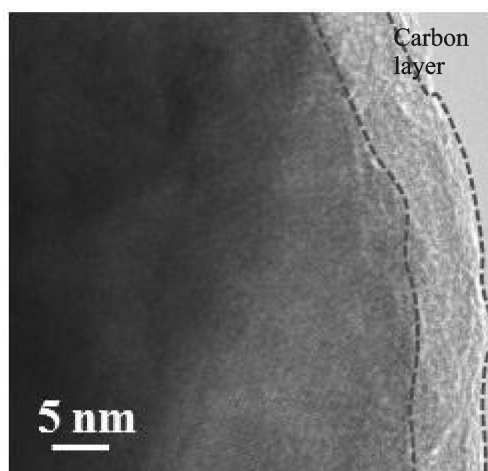

Fig. S4 TEM image of the wall of CoS_2 YS@C sphere with carbon layer thickness of ～6 nm

Fig. S5 IR-corrected polarization of CoS_2 YS@C-6 nm，CoS_2 YS@C-10 nm and CoS_2 YS@C-15 nm
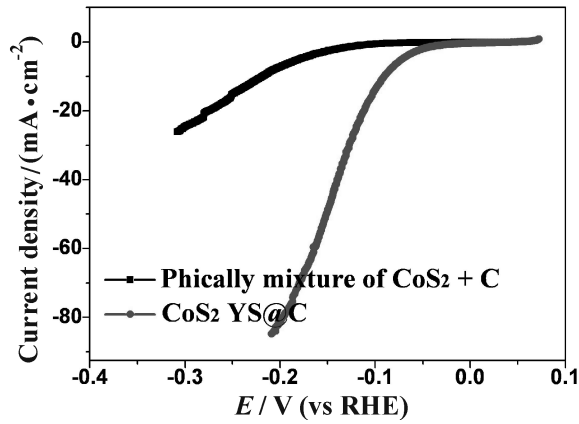
Fig. S6　IR-corrected polarization of CoS₂ YS @ C spheres and the physically mixture of CoS₂ +C
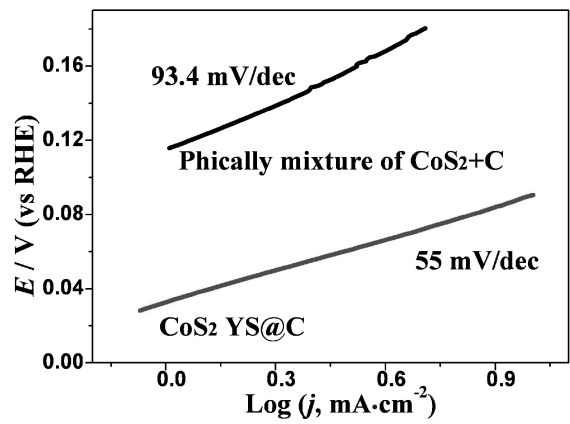

Fig. S7　Tafel curves of CoS₂ YS@C spheres and the physically mixture of CoS₂ +C
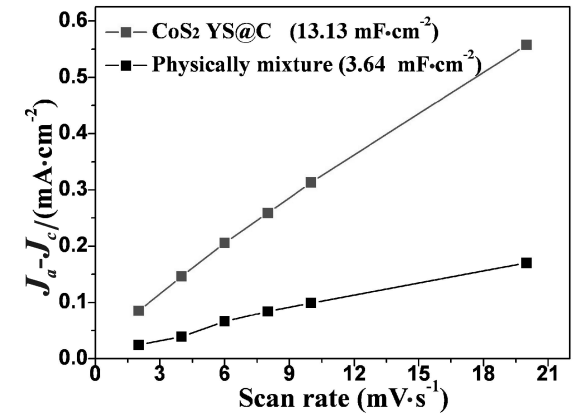

Fig. S8　Capacitive current densities at 0. 04 V as a function of scan rate for CoS₂ YS@ C and CoS₂ +C
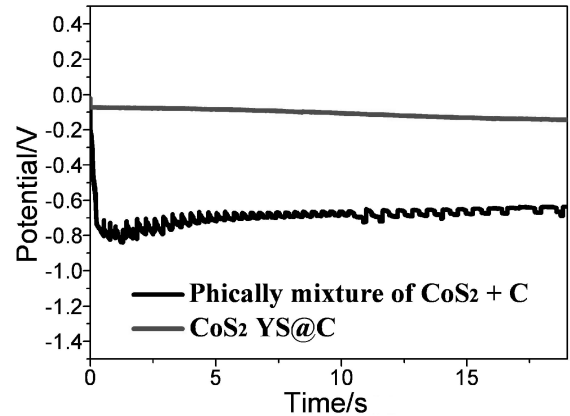

Fig. S9　Stability tests of CoS₂ YS@C and CoS₂ +C at the current density of 10 mA · cm⁻²
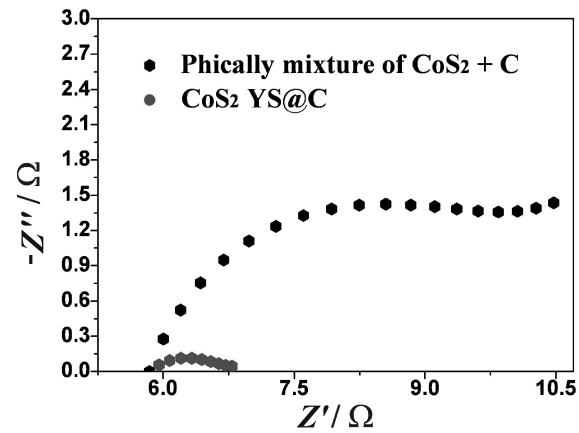

Fig. S10　Nyquist plots of CoS₂ YS@C and the physically mixture of CoS₂ +C
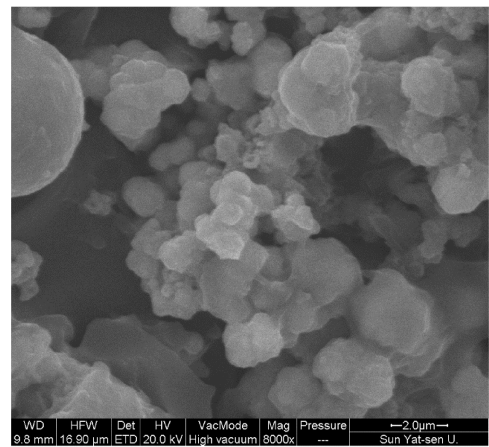

Fig. S11　SEM image of CoS₂ after chronopotentiometry mesurement

Table S1   Comparison of HER electrocatalytic activity of hollow CoS_2 YS@C spheres in acid conditions vis-à-vis other reported CoS_2 or CoS_2-based HER electrocatalysts

Electrocatalysts	The overpotentials at 10 mA · cm^{-2}/mV	Exchange current densities/ (mA · cm^{-2})	Tafel slopes/ (mV · dec^{-1})	Loadings/ (mg · cm^{-2})	Electrolytes	References
CoS_2 YS@C	90	0.265	55	1.02	0.5 M H_2SO_4	This work
CoS_2 films	190	0.00197	51.4	N. A.	0.5 M H_2SO_4	2
CoS_2 MWs	158	0.0188	58	25 ± 2	0.5 M H_2SO_4	2
CoS_2 NWs	145	0.0151	51.6	1.7 ± 0.3	0.5 M H_2SO_4	2
$MoS_2/CoS_2/CC$	87	N. A.	73.4	18.6	0.5 M H_2SO_4	3
CoS_2/CC	288	N. A.	210.7	16.5	0.5 M H_2SO_4	3
$Co(S_{0.73}Se_{0.27})_2$ NWs	104	N. A.	45.3	2.37	0.5 M H_2SO_4	4
CoS_2 nanowires		N. A.	47.1	2.24	0.5 M H_2SO_4	4
CoS_2/RGO-CNTs	142	N. A.	51	1.15	0.5 M H_2SO_4	5
CoS_2 thin films	192	N. A.	52	N. A.	0.5 M H_2SO_4	6
CoS_2/RGO nanosheets	143	N. A.	285	N. A.	0.5 M H_2SO_4	7
$CoS_{2x}Se_{2(1-x)}$ NWs arrays	129.5	N. A.	44	N. A.	0.5 M H_2SO_4	8
CoS_2 NWs	253	0.47	68.7	N. A.	0.5 M H_2SO_4	8
P-doped CoS_2 nanosheets	67	0.20	50	2.5 ± 0.1	0.5 M H_2SO_4	9
CoS_2 nanosheets	98	N. A.	58	2.0 ± 0.1	0.5 M H_2SO_4	9

N. A. represents the unknown data

References：

［1］ WANG Q, JIAO L, HAN Y, et al. CoS_2 hollow spheres: fabrication and their application in lithium-ion batteries. The Journal of Physical Chemistry C, 2011, 115, 8300.

［2］ FABER M S, DZIEDZIC R, LUKOWSKI M A, et al. High-performance electrocatalysis using metallic cobalt pyrite (CoS2) micro-and nanostructures. Journal of the American Chemical Society, 2014, 136, 10053.

［3］ HUANG J, HOU D, ZHOU Y, et al. MoS_2 nanosheet-coated CoS_2 nanowire arrays on carbon cloth as three-dimensional electrodes for efficient electrocatalytic hydrogen evolution. Journal of Materials Chemistry A, 2015, 3, 22886.

［4］ WANG K, ZHOU C, XI D, et al. Component—controllable synthesis of $Co(S_xSe_{1-x})_2$ nanowires supported by carbon fiber paper as high-performance electrode for hydrogen evolution reaction. Nano Energy, 2015, 18, 1.

［5］ PENG S, LI L, HAN X, SUN W, et al. Cobalt sulfide nanosheet/graphene/carbon nanotube nanocomposites as flexible electrodes for hydrogen evolution. Angewandte Chemie, 2014, 126(46): 12802-12807

［6］ FABER M S, LUKOWSKI M A, DING Q, et al. Earth—abundant metal pyrites (FeS_2, CoS_2, NiS_2, and their alloys) for highly efficient hydrogen evolution and polysulfide reduction electrocatalysis. The Journal of Physical Chemistry C, 2014, 118, 21347.

［7］ XING W, ZHANG Y, XUE Q, et al. Highly active catalyst of two-dimensional CoS_2/graphene nanocomposites for hydrogen evolution reaction. Nanoscale research letters, 2015, 10, 1.

［8］ LIU K, WANG F, XU K, et al. $CoS_{2x}Se_{2(1-x)}$ nanowire array: an efficient ternary electrocatalyst for the hydrogen evolution reaction. Nanoscale, 2016, 8, 4699.

［9］ OUYANG C, WANG X, WANG S. Phosphorus-doped CoS_2 nanosheet arrays as ultra-efficient electrocatalysts for the hydrogen evolution reaction. Chemical Communications, 2015, 51, 14160.